Chemical Science

ROYAL SOCIETY OF CHEMISTRY

EDGE ARTICLE

View Article Online
View Journal | View Issue

Cite this: *Chem. Sci.*, 2026, **17**, 6086

All publication charges for this article have been paid for by the Royal Society of Chemistry

Received 20th November 2025
Accepted 23rd January 2026

DOI: 10.1039/d5sc09098a

rsc.li/chemical-science

Allosteric ligand–aptamer complexes orchestrate supramolecular or transient catalytic, transcription and fibrinogenesis processes

Diva Froim, [a] Hadar Amartely, [b] Jiantong Dong, *[a] Eli Pikarsky [c] and Itamar Willner *[a]

Allosteric regulation, the modulation of biological macromolecular function through binding of molecules at distant sites distinct from the active site, is a fundamental principle in biology that governs enzyme activity, signaling, and gene expression. In this work, we present allosteric ligand/aptamer complexes, coupled to biocatalytic reaction modules composed of enzymes, DNAzymes, or transcription machineries, regulating the catalytic and transient functions of these frameworks. This principle is exemplified by the assembly of ligand/aptamer subunits supramolecular complexes that allosterically stabilize the Mg^{2+}-dependent DNAzyme, allowing its ribonucleobase cleavage activity, promoting the formation of transcription templates that yield RNA products, and modulating the assembly of thrombin aptamer subunits that inhibit thrombin-induced coagulation. Specifically, melamine (Mel)/aptamer subunits complexes allosterically stabilize the assembly of Mg^{2+}-dependent DNAzyme strands for substrate cleavage, the formation of thrombin aptamer subunits that inhibit the conversion of fibrinogen to fibrin, and the stabilization of a transcription template encoding the Malachite Green (MG) RNA aptamer. Furthermore, coupling an enzyme that depletes the ligand/aptamer complex, which allosterically stabilizes the biocatalytic reaction module, demonstrates the dissipative and transient operation of the catalytic system. This concept is illustrated by the adenosine (Ade)/aptamer subunits supramolecular complex, which stabilizes thrombin aptamer subunits to inhibit thrombin-induced fibrinogenesis, and promotes the formation of an active transcription template for RNA synthesis. In the presence of adenosine deaminase (ADA), Ade is transformed into inosine, which lacks affinity for the aptamer subunits, thereby degrading the Ade/aptamer assemblies and depleting the allosteric complexes. The temporal disassembly of these allosteric stabilizing complexes leads to the transient inhibition of thrombin-induced coagulation or to the transient operation of a transcription machinery.

Introduction

Allosteric regulation, the modulation of the activity of macromolecules through binding of molecules at distant sites, is a fundamental principle governing biological processes. The communication between spatially separated molecular domains, provides the dynamic flexibility that underlies metabolism, signaling, and gene expression.[1,2] Jacques Monod famously referred to allostery as the "second secret of life", emphasizing its central role in the self-organization and adaptability of biological systems.[3] Introduction of the allostery concept into synthetic nucleic acid structures might add an important dimension to the functional properties of the biopolymer and expand its application in synthetic biology. The base sequence comprising nucleic acids encodes functional information into the structure of the biopolymer. Sequence guided functions of DNA include sequence-specific recognition and binding of biomolecules or low molecular-weight ligands (aptamers),[4–6] sequence dictated displacement of duplex nucleic acids or protein/nucleic acid complexes by auxiliary strands,[7–9] and sequence regulated catalytic properties in the presence of auxiliary cofactors (DNAzymes or ribozymes), *e.g.*, metal-ion or amino acid-dependent DNAzymes[10–13] and hemin/G-quadruplex[14] DNAzymes. Moreover, the sequences comprising DNA duplex frameworks dictate selective reactivity patterns towards auxiliary enzymes such as endonucleases[15,16] or nickases.[17] In addition, auxiliary enzymes such as DNA or RNA polymerases and added deoxyribonucleotide triphosphates (dNTPs) or ribonucleotide triphosphates (NTPs) as fuels, catalyze in the presence of nucleic acid templates dictated polymerization and displacement of DNA or RNA products.[18,19] This arsenal of

[a]*Institute of Chemistry, The Hebrew University of Jerusalem, Jerusalem 91904, Israel. E-mail: jtdong2025@nankai.edu.cn; itamar.willner@mail.huji.ac.il*

[b]*Wolfson Centre for Applied Structural Biology, The Hebrew University of Jerusalem, Jerusalem 91904, Israel*

[c]*The Lautenberg Center for Immunology and Cancer Research, IMRIC, The Hebrew University of Jerusalem, Jerusalem 91120, Israel*

recognition and catalytic functions embedded in oligonucleotides provides a versatile "tool-box" for the rapidly developing area of DNA nanotechnology.[20] Over the years, the functional information embedded in nucleic acids has been implemented to develop DNA switches,[21,22] machines[23,24] and two- and three-dimensional DNA nanostructures.[25,26] In addition, dynamically reconfigured nanostructures,[27] programmed logic gate circuits,[28] dynamic reconfigurable DNA networks,[29] dissipative circuits,[30,31] and switchable transcription machineries[32,33] were demonstrated. Moreover, chemical modifications of aptamers with light responsive[34] or redox active units[35] led to switchable binding properties of aptamers. Conjugation of aptamers to DNAzyme catalytic units yielded hybrid structures, "nucleoaptazymes", emulating native enzymes by providing cooperative substrate binding sites in spatial proximity to the active site in the conjugated structure.[36,37] Diverse applications of aptamers were demonstrated, including their use as sensing[38,39] and imaging materials,[40] engineering of stimuli-responsive drug-carriers, and their targeting to specific cell receptors.[41] Also, aptamers were used as therapeutic agents through selective binding to proteins and their inhibition, *e.g.*, association to VEGF (inhibiting angiogenesis)[42,43] or thrombin (inhibiting fibrinogenesis).[44] Similarly, DNAzymes have found broad applications as amplifiers of sensing events, using *in vitro* or *in vivo* assays[45] and catalyzing diverse chemical transformations, such as oxidation of NADH[46] or dopamine.[47] Also, DNAzymes were employed as synthetic catalysts for gene therapy[48] and for the generation of reactive oxygen species for chemo dynamic cancer therapy.[49]

Here we wish to report on the conjugation of ligand/aptamer supramolecular complexes to DNAzyme subunits, anti-protein (thrombin) aptamer subunits and transcription templates, resulting in the allosteric operation of a DNAzyme, inhibition of fibrinogenesis and RNA transcription. Melamine (Mel) or adenosine (Ade) act as ligands assembling ligand/aptamer supramolecular complexes that allosterically guide the respective catalytic, fibrinogenic and transcription circuits. By coupling adenosine deaminase (ADA) to the Ade aptamer allosterically stabilized fibrinogenesis and transcription circuits, transient, dissipative, operation of the frameworks is achieved. Beyond the expansion of the functionalities of stimuli-responsive nucleic acid circuits, the significance of the ligand/aptamer complex, allosterically-driven, catalytic circuits is reflected by: (i) their possible application for sensing (*e.g.*, Mel); (ii) the temporal, dose-controlled, therapeutic applications of the circuits (*e.g.*, inhibition of thrombin-induced fibrinogenesis); and (iii) the spatiotemporal control-over transcription machineries by synthetic ligand/aptamer complexes emulating functions of native transcription factors. It should be noted that in a previous study[50] we reported on the allosteric adenosine/aptamer subunits activation of the Mg^{2+}-ion-dependent DNAzyme and its ADA-directed transient catalytic modulation in liposome protocells. The present study demonstrates, however, the versatility of the allosteric activation of diverse supramolecular and transient catalytic transformations such as fibrinogenesis or transcription machineries, using different ligand/aptamer subunits complexes as allosteric stabilizing units.

Results and discussion

The general concept to allosterically operate catalytic circuits consisting of DNAzymes, anti-protein (thrombin) aptamer subunits or transcription machineries by ligand/aptamer complexes is exemplified in Fig. 1A using melamine (Mel)/aptamer complexes.[51,52] The system consists of two strands A_m and B_m that include engineered sub-domains l_1 and l_2 corresponding to aptamer subunits conjugated to the catalytic subunits k_1 and k_2. The catalytic subunits include the pre-engineered sequences to operate a DNAzyme, bind thrombin or, transcribe RNA sequences. While the strands A_m and B_m have partial complementarity, it is insufficient to form a stable interstrand complex. However, binding of the ligand (Mel) to the aptamer subunits results in an interstrand supramolecular complex cooperatively stabilized by the ligand/aptamer complex and the complementarity associated with the two strands. Furthermore, the spatial proximity between the tethers k_1 and k_2 is pre-engineered to evolve the catalytic function in the supramolecular assembly. That is, the ligand-induced formation of ligand/aptamer supramolecular complex allosterically stabilizes and activates the catalytic function of the spatially confined k_1 and k_2 subunits.

Fig. 1B schematically depicts the Mel/aptamer subunits complex induced allosteric stabilization of a supramolecular complex activating the function of a Mg^{2+}-ion-dependent DNAzyme. The reaction circuit includes two strands D_m and E_m which include subunits b_1 and b_2 of the split Mel aptamer, and subunits m_1 and m_2 corresponding to the arm/loop sequences of the DNAzyme. The complementary sequence domains a and a′ were added to strands D_m and E_m. In the presence of Mel, the supramolecular complex cooperatively stabilized by the Mel/aptamer subunits complex and the inter-bridging duplex a/a′ is formed, resulting in the spatially confined DNAzyme configuration composed of m_1 and m_2. The allosteric stabilization of the functional Mg^{2+}-ion-dependent DNAzyme is then probed by the cleavage of the fluorophore/quencher modified substrate S by the DNAzyme, panel I (F = FAM; Q = BHQ1). For the specific design of the structural units activating the allosteric Mel-induced operation of the DNAzyme see Page S9 in the SI.

Fig. 1C, depicts the rate of cleavage of the F/Q-modified substrate by the allosterically, Mel-stabilized DNAzyme framework in the presence of variable Mel concentrations. While no cleavage of the substrate proceeds in the absence of Mel, consistent with the lack of communication between strands D_m and E_m, curve i, the supramolecular DNAzyme structure is activated in the presence of Mel, curves ii–xii. As the concentration of Mel increases, the rate of cleavage is enhanced. Fig. 1D, displays the rates of cleavage of the substrate strand in the presence of variable Mel concentrations. A saturation curve is observed consistent with the saturated formation of the Mel/aptamer subunits complex from which the $V_{max} = 2.41 \pm 0.07$ μmol min^{-1} and $K_{0.5} = 162 \pm 4.8$ μM for the allosterically stabilized supramolecular DNAzyme were evaluated. The detection limit of the DNAzyme was calculated to be 867 ±

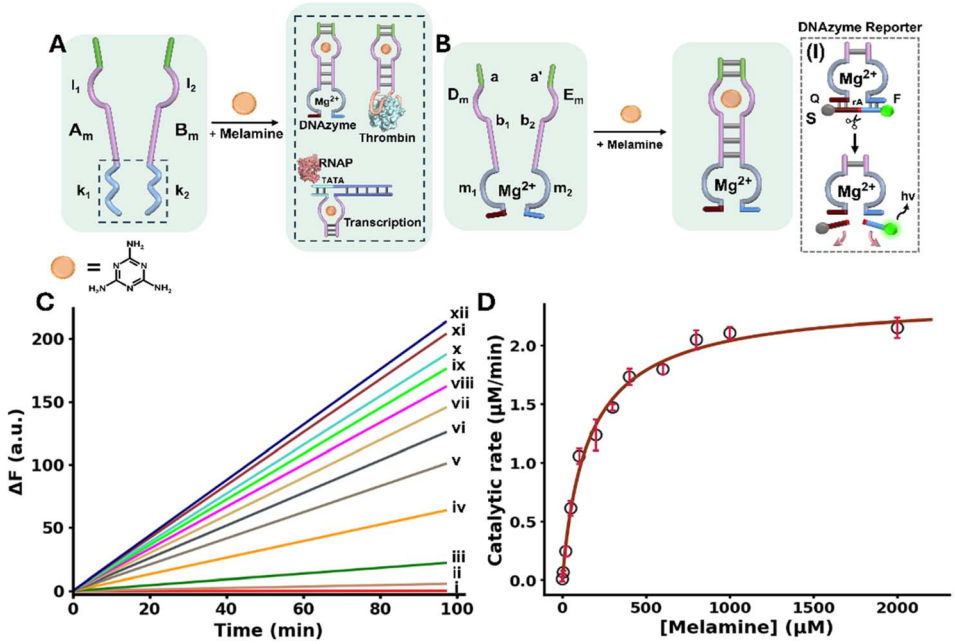

Fig. 1 (A) Allosteric activation of catalytic DNA circuits by supramolecular assembly of ligand/aptamer subunits complexes using melamine (Mel)/aptamer subunits. (B) Schematic Mel-induced allosteric stabilization of a Mg^{2+}-ion-dependent DNAzyme through Mel/aptamer subunits complex. Panel I – probing the catalytic activity of the DNAzyme by the DNAzyme-catalyzed ribonucleobase cleavage of a fluorophore (FAM)/quencher (BHQ1)-modified substrate strand, S. (C) Time-dependent fluorescence changes upon cleavage of the F/Q-modified substrate by the allosterically-stabilized DNAzyme formed in the presence of variable concentrations of Mel: (i) 0 μM, (ii) 5 μM, (iii) 20 μM, (iv) 50 μM, (v) 100 μM, (vi) 200 μM, (vii) 300 μM, (viii) 400 μM, (ix) 600 μM, (x) 800 μM, (xi) 1000 μM, (xii) 2000 μM. (D) Catalytic rates of the allosterically stabilized DNAzyme, in the presence of variable concentrations of Mel (fluorescence intensities were translated to free fluorophore concentration using the appropriate calibration curve, Fig. S1).

26 nM using the three-sigma method. Isothermal titration calorimetry (ITC) experiments supported the Mel/aptamer subunits formation of the supramolecular DNAzyme structure revealing a K_d of 0.890 ± 0.123 μM corresponding to the complex between Mel and the two subunits D_m and E_m, Fig. S2. Beyond demonstrating the Mel/aptamer induced allosteric activation of the Mg^{2+}-ion-dependent DNAzyme, the system presents as an amplified Mel sensing platform. Mel sensing is of importance as Mel has been used as an illegal additive in food products causing severe health problems in infants.[53] Different analytical methods including mass-spectrometry,[54] high performance liquid chromatography[55] and CRISPR/Cas14a sensing platforms[56] were developed to detect Mel residues in food products. The amplified Mel-dependent operation of the DNAzyme allows the analysis of Mel with a detection limit corresponding to 0.1 ppm, that is lower than the detection threshold defined by the FDA for infant formula (1.0 ppm).[57]

The allosteric Mel/aptamer subunits complex stimulating the catalytic functions of a conjugated DNA framework were further demonstrated with the Mel-mediated inhibition of fibrinogen to fibrin coagulation. Thrombin is a key physiological regulator of the blood clotting mechanism.[58] While it plays a key role in hemostatic clotting of vascular injuries, its balanced dose activity is crucial to prevent blood clots and thrombosis.[59,60] Diverse anti-coagulant therapeutic agents, controlling thrombin activity are known.[61] Within these efforts, anti-thrombin aptamers that bind to thrombin were isolated and their inhibition of thrombin was implemented to design anti-coagulant agents.[62,63] The dose-controlled, inhibition of thrombin catalytic functions by aptamers, acting as anti-coagulation agents, could thus be a significant advance in controlling blood clotting (thrombosis). Accordingly, the allosteric activation of the blood clotting inhibitory capacity of the anti-thrombin aptamer framework using an auxiliary ligand, *e.g.* Mel, could be an interesting path to follow. This concept is exemplified in Fig. 2A with the design of a Mel/aptamer subunits allosteric circuit for the controlled inhibition of thrombin's coagulation function.

The system consists of two strands G_m and H_m composed of the subsequences b_1 and b_2 corresponding to the Mel aptamer subunits, extended by four base complementary tethers, a and a′, cooperatively enhancing the stability of the Mel/aptamer subunits complex. The Mel aptamer subunits G_m and H_m are further extended by the tethers t_1 and t_2 that correspond to the anti-thrombin aptamer subunits. Despite the partial complementarity of strands G_m and H_m and the binding affinity of thrombin to the subunits t_1 and t_2, the strands G_m and H_m lack binding affinity to allow the formation of the G_m/H_m/thrombin complex, and thus, the inhibition of thrombin-induced fibrinogenesis (coagulation of fibrinogen to fibrin) is prohibited. The rate of thrombin-induced coagulation in the absence of the strands G_m/H_m yet in the presence of Mel, is reflected by the temporal light-scattering of the system, show similar temporal light-scattering intensity changes to free

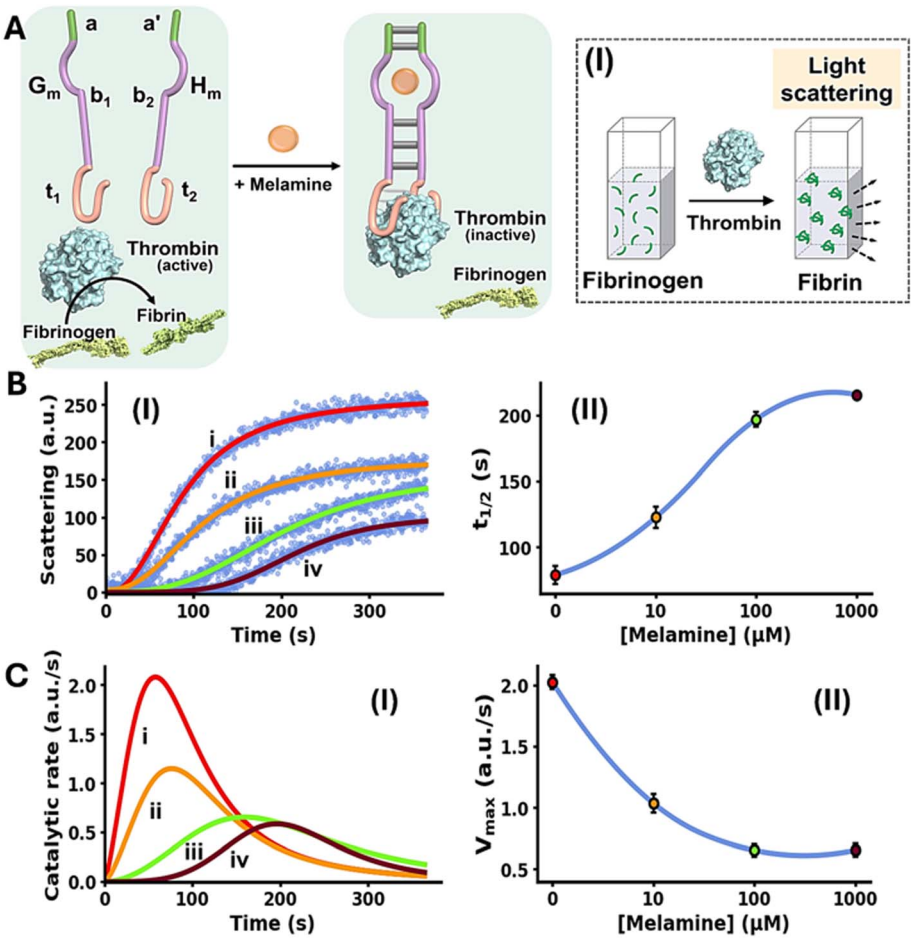

Fig. 2 (A) Schematic melamine (Mel)-induced allosteric inhibition of thrombin-induced fibrinogenesis (conversion of fibrinogen to fibrin) through the formation of thrombin/thrombin aptamer subunits framework. Panel I – schematic probing of the fibrinogenesis process by dynamic light-scattering. (B) Panel I – temporal light-scattering curves upon inhibition of thrombin-induced fibrinogenesis in the presence of the thrombin/Mel aptamer subunits framework G_m/H_m and variable concentrations of Mel: (i) 0 μM, (ii) 10 μM, (iii) 100 μM, (iv) 1000 μM. Panel II – $t_{1/2}$ values derived from fibrinogenesis temporal light-scattering curves, in the presence of variable concentrations of Mel. (C) Panel I – temporal catalytic rates of thrombin-induced fibrinogenesis in the presence of G_m/H_m strands, allosterically stabilized by variable concentrations of Mel: (i) 0 μM, (ii) 10 μM, (iii) 100 μM, (iv) 1000 μM. Panel II – maximum fibrinogenesis rates (V_{max}) upon subjecting G_m/H_m to variable concentrations of Mel. In all experiments, $G_m/H_m = 1.0$ μM, thrombin = 5 nM, fibrinogen = 10 mg ml^{-1}. Data are means ±SD, $N = 3$.

thrombin in the absence of ligands, Fig. S4. The allosteric Mel/aptamer subunits stabilization of the thrombin/anti-thrombin subunits results in the Mel-induced, controlled inhibition of the thrombin-induced coagulation of fibrinogen to fibrin. The rate of fibrinogenesis is followed by the temporal light-scattering features associated with the coagulation of fibrinogen to fibrin, in the presence of variable Mel concentrations, Fig. 2A, panel I. Fig. 2B, panel I, depicts the time-dependent light-scattering intensity changes associated with the thrombin-induced coagulation of fibrinogen to fibrin in the presence of strands G_m and H_m, in the absence of Mel, curve (i), and in the presence of variable concentrations of Mel, curves (ii)–(iv). While in the absence of Mel rapid fibrinogenesis is observed, the addition of Mel induces the formation of inter-strand Mel/G_m/H_m and the coagulation of fibrinogen to fibrin is suppressed, thus as the concentration of Mel increases the degree of inhibition of fibrinogenesis is higher. The temporal light-scattering curves probing the allosteric inhibition efficacy of fibrinogenesis, in the presence of variable concentrations of Mel were quantitatively evaluated using two parameters.[64,65] One parameter, $t_{1/2}$, is the time interval corresponding to the light-scattering intensity reaching 50% of the saturation value at variable concentrations of Mel. Fig. 2B, panel II, depicts the relation of $t_{1/2}$ to the concentrations of Mel inducing allosterically the inhibition of thrombin. As the concentration of Mel increases the $t_{1/2}$ light-scattering intensity values are higher reflecting an enhanced thrombin inhibition capability of the circuit. A second parameter evaluating the Mel-induced inhibition of thrombin is the maximum coagulation rates of fibrinogen to fibrin (V_{max}) that are derived from the temporal light-scattering curves in the presence of variable Mel concentrations, first order time-dependent derivative curves are shown in Fig. 2C, panel I. The V_{max} values of the circuit, characterizing the inhibition efficacy induced by Mel, derived from the temporal light-scattering curves shown in Fig. 2B, panel I, are displayed in Fig. 2C, panel II. While a high V_{max} in the absence

of Mel is observed, reflecting low thrombin inhibition, the V_{max} values decrease as the concentration of Mel increases, demonstrating the enhanced efficiency of Mel-induced inhibition of coagulation of fibrinogen to fibrin. The results displayed in Fig. 2 introduce a new paradigm for controlling thrombin-induced coagulation by employing an auxiliary ligand (Mel) that allosterically regulates the dose-controlled formation of the thrombin/anti-thrombin aptamer subunits affinity complex that inhibits the coagulation process.

In the next step, the allosteric Mel-induced activation of a transcription machinery was examined. Regulation of RNA transcription controls many biological processes ranging from cell cycle progression[66] and maintenance of intracellular metabolism to cellular differentiation.[67] The transcription apparatus demonstrates dynamic adaptive features, primarily modulated by transcription factors.[68–71] Beyond the key functions of the native transcription machinery in maintenance of living organisms, misregulation of transcription programs by dysfunctional transcription factors is the origin of various diseases including cancer, viral infection, neurological disorders, autoimmune pathologies and diabetes.[72,73] Development of biomimetic synthetic transcription circuits is important not only to emulate the native apparatus by artificial model systems, but it could provide versatile therapeutic applications. For example, the controlled programmed *in vivo* synthesis of pre-engineered RNA could be a valuable source of therapeutic agents, *e.g.* aptamers, siRNAs, and ribozymes. Indeed, recent research efforts demonstrated the modulation of transcription machineries by topological nucleic acid barriers conjugated to transcription templates, such as G-quadruplexes or DNA triplexes modeling native transcription factors' functions.[64] In the forthcoming section we introduce the allosteric Mel-induced operation of a transcription circuit as a biomimetic model system emulating the functions of transcription factors.

The Mel/aptamer subunits complex triggered activation of the transcription machinery is schematically displayed in Fig. 3A. The inactive reaction module consists of the template strands N_m/T_m containing an incomplete T7 RNA polymerase (RNAP) promoter, the strand P_m, Malachite Green (MG) and T7 RNAP/ribonucleotide triphosphates (NTPs) mixture. The strands T_m and P_m include tethers b_1 and b_2 corresponding to the Mel aptamer subunits, where b_1 is extended by the sequence x′ that is complementary to domain x in the template N_m/T_m. While x′ contains the sequence to complete the promoter region that activates the N_m/T_m transcription machinery, the stability of the complementary duplex x/x′ is, however, insufficient to activate the transcription machinery. In the presence of Mel, the cooperative formation of the Mel/aptamer subunits complex, and the duplex x/x′ form an energetically stabilized, promoter-activated, transcription template enabling the activation of the transcription machinery, resulting in the T7 catalyzed RNAP/NTPs transcription of the RNA product, R_1. The template N_m/T_m is pre-engineered to yield the MG RNA aptamer as the transcription product. The resulting fluorescent MG/RNA aptamer complex (λ_{ex} = 632 nm; λ_{em} = 650 nm) provides, then, an optical readout signal for the temporal operation of the transcription machinery. Fig. 3B depicts the time-dependent fluorescence changes caused by the production of the MG RNA aptamer product, generated in the absence of Mel, curve i, and in the presence of variable concentrations of Mel, curves ii–vi. Using an appropriate calibration curve, relating the fluorescence intensity of MG/RNA aptamer to its concentration, Fig. S5, the rates of MG/RNA aptamer formation as a function of Mel concentrations were evaluated as depicted in Fig. 3C. Peak rates (V_{max}) of the transcription template derived from Fig. 3C are displayed in Fig. 3D, as Mel concentration increases, V_{max} increases.

The systems discussed so far demonstrated the allosteric ligand (Mel)-induced activation of catalytic processes involving a DNAzyme, thrombin-induced fibrinogenesis or a transcription machinery. Many of the catalytic processes in nature are, however, temporally modulated, leading to dissipative, transient and out-of-equilibrium operation.[74] The ligand/aptamer complex allosterically regulating catalytic processes introduced a mechanism controlling the "dose" of the catalytic transformation. The coupling of a catalyst modulating temporally and transiently the allosteric mechanism could introduce an additional dimension to the "dose" regulated control over catalytic processes. The principle of dissipative out-of-equilibrium systems involves the design of reaction circuits that are activated by an auxiliary energy-fueled input (chemical fuel, light, electrical or magnetic stimuli) that generate an intermediate out-of-equilibrium state. The system includes, however, an internal mechanism depleting the auxiliary energy-fueled input resulting in the degradation of the intermediate state, into waste products while recovering the parent circuit. This leads to the temporal, transient, formation and depletion of the intermediate state. Substantial recent research efforts addressed the use of nucleic acid-based frameworks as functional reaction modules to design transient DNA circuits.[75,76] Different triggers including nucleic acid fuel strands or light coupled to enzymes or DNAzymes were employed to trigger the temporal transitions of DNA frameworks into intermediate states that are temporally depleted by the catalysts to the parent reaction modules, thereby establishing transiently operating DNA circuits.[77,78] Diverse applications of transient operating circuits were demonstrated, including transient operating biocatalytic cascades,[79] transient DNA-based load release systems,[80] or transient nucleic acid guided aggregation/de-aggregation of metal nanoparticles or semiconductor quantum dots.[81] The allosteric ligand/aptamer stabilization of catalytic frameworks, and the availability of enzymes degrading the ligands, suggests that coupling of enzymes to the allosterically ligand/aptamer stabilized catalytic frameworks could provide a versatile mechanism to engineer dynamic, transient allosterically ligand-stabilized reaction modules. For example, diverse ligand/aptamer complexes can be coupled with ligand degrading enzymes (*e.g.*, adenosine/adenosine deaminase, acetylcholine/acetylcholinesterase, uric acid/uricase) resulting in the separation of the complexes, as schematically shown in Fig. S6.

The conjugation of an enzyme to an allosteric ligand-induced catalytic transformation leading to transient allosterically-driven catalytic process is schematically presented

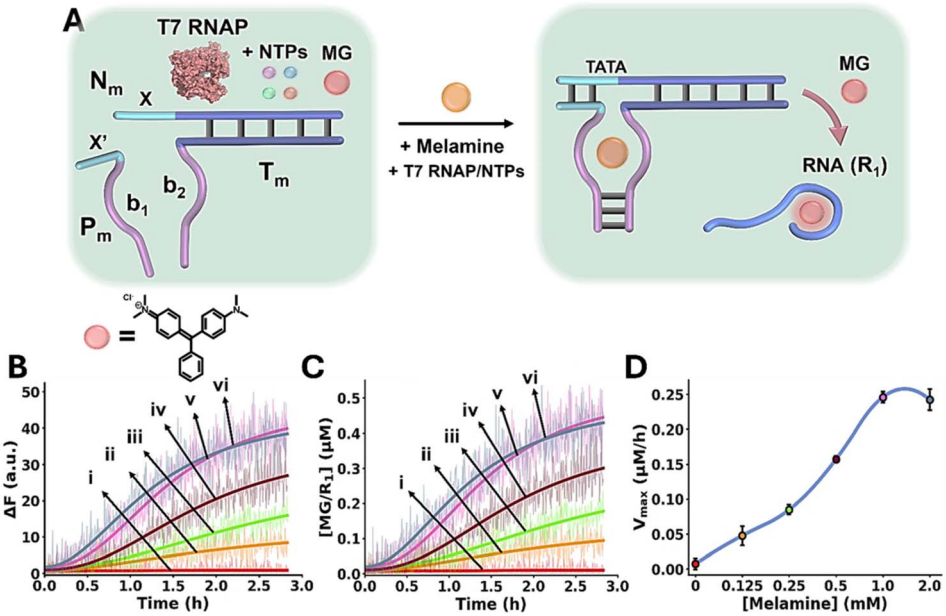

Fig. 3 (A) Schematic melamine (Mel)/aptamer subunits allosterically triggering of the transcription machinery transcribing the Malachite Green (MG) RNA aptamer. The fluorescent MG/aptamer complex provides the readout signal for the transcription process. (B) Time-dependent fluorescence changes of the MG/RNA aptamer transcribed product generated in the presence of variable concentrations of Mel: (i) 0 mM, (ii) 0.125 mM, (iii) 0.25 mM, (iv) 0.5 mM, (v) 1.0 mM, (vi) 2.0 mM. (C) Temporal concentration changes of the MG/RNA aptamer transcribed product generated in the presence of variable concentrations of Mel: (i) 0 mM, (ii) 0.125 mM, (iii) 0.25 mM, (iv) 0.5 mM, (v) 1.0 mM, (vi) 2.0 mM (translation of the temporal fluorescence changes shown in (B) to MG/aptamer concentrations were performed using the calibration curve provided in Fig. S5). (D) Maximum catalytic rates (V_{max}) corresponding to the formation of the transcribed MG/aptamer product, in the presence of variable Mel concentrations. In all experiments, $N_m/T_m = 0.2$ μM, $P_m = 0.2$ μM, NTPs = 0.5 mM, T7 RNAP = 1.5 U μl^{-1}. Data are means ±SD, $N = 3$.

in Fig. 4A, using the adenosine (Ade)/aptamer subunits complex and adenosine deaminase (ADA) as regulators controlling allosteric catalytic processes such as fibrinogenesis or transcription (for the design principles of the allosteric Ade/aptamer subunits inhibition of thrombin see Fig. S3 and accompanying discussion Page S11 in the SI). The two strands A_a and B_a coupled with ADA, act as the reaction module. The strands A_a and B_a include the Ade aptamer subunits l_3 and l_4 conjugated to strands k_1 and k_2 that encode the nucleic acid sequences comprising the catalytic frameworks. Fueling the system with Ade results in the formation of Ade/aptamer subunits supramolecular complex allosterically stabilizing the catalytic frameworks consisting of the thrombin/anti-thrombin aptamer subunits complex inhibiting fibrinogenesis, or the active transcription machinery as intermediate products. The ADA present in the system concomitantly transforms Ade to inosine, that lacks affinity towards the aptamer subunits. Separation of the Ade/Ade aptamer complex recovers the parent reaction circuit, in which the catalytic transformations are prohibited. This leads to the transient Ade/ADA allosteric operation of fibrinogenesis or transcription processes. In the forthcoming section, the transient Ade/ADA operation of transcription and fibrinogenesis machineries will be addressed.

Fig. 4B depicts schematically the reaction circuit used for the allosteric transient inhibition of the thrombin-induced coagulation of fibrinogen to fibrin in the presence of Ade and ADA. The system consists of two strands G_a and H_a as the DNA functional framework and ADA as the auxiliary catalyst. The strands G_a and H_a include the Ade aptamer subunits d_1 and d_2 conjugated to the complementary sequences c and c′ and extended by the anti-thrombin aptamer subunits t_1 and t_2. While in the absence of Ade, the base complementarity of c and c′ is insufficient to form a stable G_a/H_a duplex structure that binds to thrombin and inhibits the thrombin-induced fibrinogenesis. The addition of Ade leads to the formation of the Ade/aptamer subunits complex, cooperatively stabilized by the c/c′ duplex, leading to the assembly of the supramolecular G_a/H_a complex that stabilizes the thrombin aptamer subunits allowing the association of the interstrand Ade/G_a/H_a supramolecular thrombin aptamer subunits framework to thrombin. Binding of the interstrand Ade/G_a/H_a to thrombin allosterically inhibits thrombin-induced fibrinogenesis. The ADA coupled to the reaction circuit, concomitantly transforms Ade to inosine, leading to the separation of the G_a/H_a units from thrombin, thereby recovering the free thrombin, exhibiting non-inhibited coagulation rate. That is, the system reveals transient allosteric Ade-induced inhibition of thrombin-induced coagulation of fibrinogen to fibrin. The degree of inhibition is controlled by the concentration of Ade that regulates the allosteric formation of the Ade/aptamer subunits complex. While the ADA concentration dictates the rate of recovery of the parent module, showing non-inhibited fibrinogenesis. That is, the transient allosteric inhibition of thrombin is regulated by two parameters; the concentration of Ade that triggers the fibrinogenesis inhibition and the concentration of ADA degrading Ade thereby regulating the temporal depletion of the inhibition

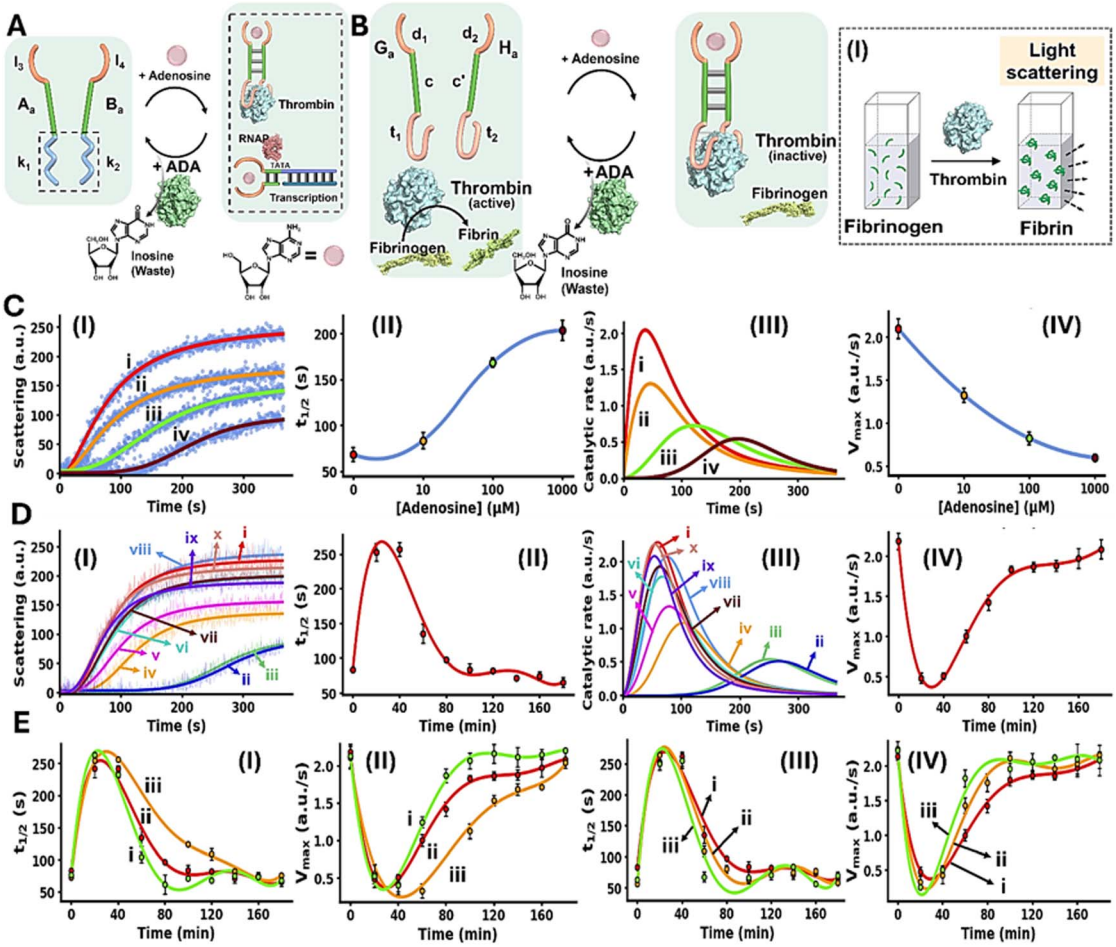

Fig. 4 (A) Allosteric transient activation of catalytic DNA systems by supramolecular assembly of ligand/aptamer subunits complexes using adenosine (Ade)/Ade aptamer and adenosine deaminase (ADA). (B) Schematic application of Ade/aptamer subunits for the Ade/ADA transient allosteric inhibition of thrombin-induced fibrinogenesis. Panel I – probing thrombin activity by following temporal light-scattering intensities associated with coagulation of fibrinogen to fibrin. (C) Panel I – light-scattering intensities upon coagulation of fibrinogen to fibrin using the reaction circuit shown in (B) operating in the presence of variable Ade concentrations, yet in the absence of ADA: (i) 0 μM, (ii) 10 μM, (iii) 100 μM, (iv) 1000 μM. Panel II – $t_{1/2}$ values of the reaction circuit in the presence of variable Ade concentrations extracted from panel I. Panel III – evaluation of the catalytic rates associated with the temporal light-scattering intensity changes, in the presence of variable concentrations of Ade: (i) 0 μM, (ii) 10 μM, (iii) 100 μM, (iv) 1000 μM. Panel IV – maximum catalytic rates (V_{max}) associated with the system's operation shown in panel III. (D) Panel I – temporal light-scattering intensities corresponding to samples withdrawn at time-intervals, from the reaction circuit displayed in (B) demonstrating transient fibrinogenesis inhibition capability in the presence of Ade = 1.5 mM; ADA = 0.045 U ml^{-1}, after: (i) 0, in the absence of Ade, (ii) 20, (iii) 40, (iv) 60, (v) 80, (vi) 100, (vii) 120, (viii) 140, (ix) 160, (x) 180 minutes. Panel II – analysis of temporal $t_{1/2}$ values corresponding to transient fibrinogenesis induced by the reaction module shown in (B), Ade = 1.5 mM; ADA = 0.045 U ml^{-1}. Panel III – analysis of the temporal catalytic rates of the temporal light-scattering intensities shown in panel I, of the transient fibrinogenesis induced by the reaction circuit displayed in (B), Ade = 1.5 mM; ADA = 0.045 U ml^{-1}. Panel IV – transient V_{max} values derived from panel III. (E) Panels I and II – transient fibrinogenesis driven in the presence of ADA = 0.045 U ml^{-1} and different concentrations of Ade: (i) 1.25 mM, (ii) 1.5 mM, (iii) 1.8 mM, displayed using $t_{1/2}$ and V_{max} parameters. Panels III and IV – transient fibrinogenesis driven in the presence of Ade = 1.5 mM and different concentrations of ADA: (i) 0.045 U ml^{-1}, (ii) 0.055 U ml^{-1}, (iii) 0.065 U ml^{-1}, displayed using $t_{1/2}$ or V_{max} parameters. In all experiments, G_a/H_a = 1.0 μM, thrombin = 5 nM, fibrinogen = 10 mg ml^{-1}. Data are means ±SD, N = 3.

phenomenon. The temporal and transient allosteric inhibition of thrombin, is then, followed by the temporal light-scattering features associated with the coagulation of fibrinogen to fibrin, in the presence of variable Ade and ADA concentrations, Fig. 4B, panel I. The rate of thrombin-induced coagulation in the absence of the strands G_a/H_a, yet in the presence of Ade, show similar temporal light-scattering intensity changes to free thrombin in the absence of ligands, Fig. S4.

Fig. 4C, panel I, shows the temporal light-scattering intensities associated with the fibrinogenesis in the presence of different concentrations of Ade, yet in the absence of ADA: (i) 0 μM (ii) 10 μM (iii) 100 μM (iv) 1000 μM. As the concentration of Ade increases, the allosteric inhibition of the thrombin-induced fibrinogenesis increases as reflected by a prolonged initial lag and lower saturation values of temporal light-scattering curves. The analysis of the temporal light-scattering curves in panel I, in terms of $t_{1/2}$, temporal catalytic rates and V_{max} values are presented in Fig. 4C panels II-IV. Fig. 4D, panel I shows the temporal light-scattering curves associated with the thrombin-induced fibrinogenesis at time-intervals of the system's

operation using Ade = 1.5 mM; ADA = 0.045 U ml^{-1}. While the control of the system, curve (i), in the absence of Ade demonstrates non-inhibited fibrinogenesis, addition of Ade leads to effective inhibition of fibrinogenesis, curve (ii), the system reveals, however, a continuous temporal change in the rate of fibrinogenesis reflected by the decrease in the inhibition effect in the system and ultimately shows the recovery of the non-inhibited fibrinogenesis behavior of the system, curves (ii)–(x). Analysis of the temporal light-scattering curves shown in Fig. 4D panel I in terms of $t_{1/2}$, temporal catalytic rates and V_{max} are summarized in Fig. 4D, panels II–IV. The result demonstrates the transient allosteric Ade-induced inhibition of thrombin by Ade/ADA in the G_a/H_a reaction circuit. Fig. 4E depicts the effects of different Ade and ADA concentrations on the transient allosteric inhibition of thrombin-induced fibrinogenesis, as reflected by the $t_{1/2}$ and V_{max} values derived from the temporal light-scattering intensities in the respective G_a/H_a operating system. As the concentration of Ade increases, at fixed ADA concentration 0.045 U ml^{-1}, the time-interval of the transient recovery of the allosterically inhibited thrombin-induced fibrinogenesis is prolonged, Fig. 4E, panels I and II. In addition, as the ADA concentration increases, at a fixed Ade concentration 1.5 mM, the time-interval of the transient recovery of the non-inhibited thrombin-induced fibrinogenesis is shortened, Fig. 4E, panels III and IV. These results are consistent with the allosteric transient inhibition of the thrombin-induced coagulation of fibrinogen to fibrin regulated by the Ade/ADA-G_a/H_a reaction circuit.

An additional process demonstrating the transient allosteric activation of a biocatalytic process included the Ade/ADA allosteric transient activation of a transcription machinery. Beyond transcription factor-modulated transcription machineries and accompanying regulated gene expression, promoter control elements regulate the dynamic interactions of transcription factors with the transcription machineries. These include for example, enhancer,[82] silencer[83] or switching elements,[84] leading to temporal dynamic modulation of transcription and gene expression. For example, by coupling two mutually repressing transcription factor pathways, biomimetic oscillatory[85] or bistable[86] active gene expression were reported. Also, transient transcription machineries regulated by auxiliary enzymes[87] or DNAzymes[88] were reported. The allosteric ligand/aptamer transient activation of a transcription process is, to the best of our knowledge, unprecedented.

Fig. 5A depicts schematically the transient Ade/ADA allosteric operation of a transcription machinery. The reaction module consists of the strands N_a/T_a that exist as an inactive transcription template lacking a full T7 promoter sequence. The strand P_a contains the sequence x′ that hybridizes to the sequence x in strand N_a and completes the T7 promoter, however despite the complementarity of the domains x/x′ they are pre-engineered to form a non-stable five-base duplex. To assist the binding of P_a to the transcription template, Ade aptamer subunits, d_1 and d_2, were conjugated to strands P_a and N_a. Added Ade cooperatively stabilize the formation of the active transcription template by the cooperative formation of the Ade/aptamer subunits complex and the x/x′ duplex completing the promoter domain in the transcription template. Formation of the intact Ade-stabilized transcription template activates, then, the T7 RNAP/NTPs transcription machinery transcribing the RNA product, R_2. Since the affinity of the Ade aptamer towards other adenine-containing ligands is well established,[89] ATP was excluded from the reaction circuit. The transcription template is pre-engineered to displace, by the transcribed RNA, R_2, the auxiliary transducing F/Q DNA duplex that is comprised of a fluorophore-modified (FAM) strand and a quencher-modified (BHQ1) strand, where the fluorescent signal is effectively quenched, generating the fluorescent F/R_2 duplex and the free quencher-modified strand Q. Thus, the time-dependent fluorescence changes in the system reflect the temporal performance of the transcription process induced by Ade. The ADA integrated in the circuit, temporally transforms Ade to inosine resulting in the depletion of Ade, leading to the separation of the strand P_a from the transcription template, that transiently recovers the parent reaction circuit. Thus, the ADA present in the system induces the transient dissipative evolution of the fluorescent intermediate F/R_2 duplex in the system. The temporal fluorescence changes caused by the displacement induced by the RNA product reflect, then the dynamically modulated transcription occurring in the system. Fig. 5B, panels I–III, depict the time-dependent fluorescence changes generated by the reaction module in the presence of different concentrations of Ade, yet in the absence of ADA: (i) 0 mM (ii) 0.125 mM (iii) 0.5 mM (iv) 2.0 mM. While in the absence of Ade minimal transcription of R_2 occurs (reflected by the lack of separation of the F/Q-transducing duplex), curve i, the time-dependent fluorescence changes are intensified as the concentration of Ade increases, curves ii–iv. Using an appropriate calibration curve relating the fluorescence of the released FAM-labeled DNA strand as a function of R_2 concentration, Fig. S7, the temporal transcribed RNA product R_2 in the presence of different Ade concentrations is displayed in Fig. 5B, panel II. Temporal first order maximum catalytic rates (V_{max}) of the transcription template derived from panel II are displayed in panel III. The results confirm that Ade stabilizes allosterically the assembly of the promoter/transcription template $P_a/N_a/T_a$ transcribing the product R_2. Fig. 5C depicts the temporal fluorescence changes generated by the transcription machinery, in the presence of variable Ade concentrations and a constant concentration of ADA = 0.025 U ml^{-1}. The temporal fluorescence changes, reflecting the rate of R_2 production reveal a non-linear behavior tending to reach a saturation value. The temporal fluorescence changes and the resulting saturation levels are controlled by the concentration of Ade. As the concentration of Ade increases, the intensities of the fluorescence changes are higher, consistent with the increased concentration of the Ade/aptamer subunits stabilized active transcription template. The non-linear temporal fluorescence intensity changes support that an accompanying mechanism slowing down the transcription process exists in the system, consistent with the ADA-induced depletion of the transcription machinery. Using a calibration curve relating the fluorescence intensities to the R_2 RNA concentrations, Fig. S7, the temporal concentrations of the transcribed R_2 were evaluated, Fig. 5C,

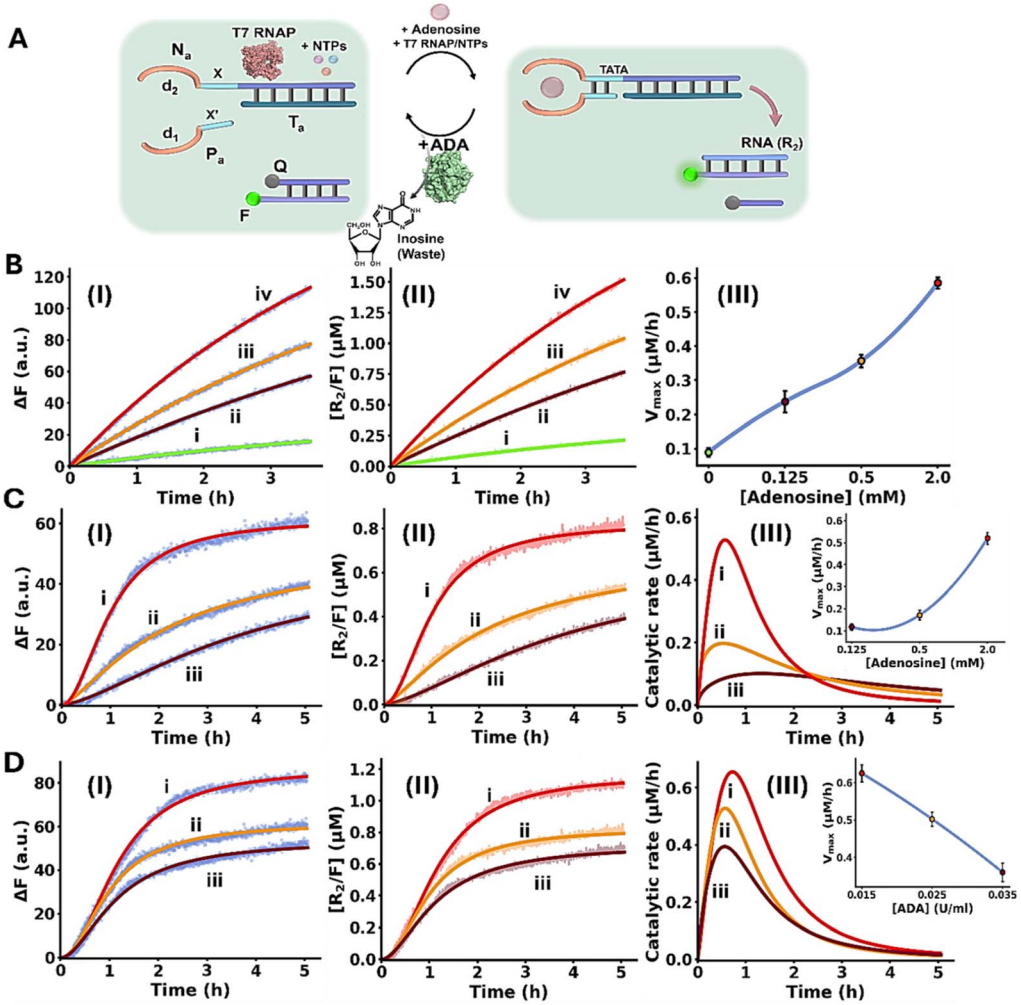

Fig. 5 (A) Panel I – schematic reaction module applying the adenosine (Ade)/adenosine deaminase (ADA) system for the transient allosteric operation of a transcription machinery emulating temporal transcription factor regulated transcription. (B) Temporal fluorescence changes generation by the Ade-driven operation of the reaction module, in the absence of ADA, and in the presence of variable Ade concentrations: (i) 0 mM, (ii) 0.125 mM, (iii) 0.5 mM, (iv) 2.0 mM. Panel II – temporal concentration changes of R_2, generated by the reaction module shown in (A), in the absence of ADA and in the presence of variable Ade concentrations: (i) 0 mM, (ii) 0.125 mM, (iii) 0.5 mM, (iv) 2.0 mM (translation of the fluorescence changes shown in panel I into R_2 concentrations, using the appropriate calibration curve, Fig. S7). Panel III – temporal catalytic rates corresponding to the generation of R_2 by the reaction module, under variable Ade concentrations. (C) Panel I – temporal fluorescence changes generated by the reaction module in the presence of ADA = 0.025 U ml^{-1} and variable concentrations of Ade: (i) 2.0 mM, (ii) 0.5 mM, (iii) 0.125 mM. Panel II – temporal concentration changes of R_2 generated by the reaction module in the presence of ADA = 0.025 U ml^{-1} and variable Ade concentrations: (i) 2.0 mM, (ii) 0.5 mM, (iii) 0.125 mM (translation of the fluorescence changes shown in panel I into R_2 concentrations, using the appropriate calibration curve, Fig. S7). Panel III – catalytic rates corresponding to the production of R_2 in the presence of ADA = 0.025 U ml^{-1}, and variable Ade concentrations: (i) 2.0 mM, (ii) 0.5 mM, (iii) 0.125 mM (first order time-dependent derivatives of the curves shown in panel II). Inset: peak rates of transient formation of R_2 at different Ade concentrations. (D) Panel I – temporal fluorescence changes generated by the reaction module in the presence of Ade = 2.0 mM and variable concentration of ADA: (i) 0.015 U ml^{-1}, (ii) 0.025 U ml^{-1}, (iii) 0.035 U ml^{-1}. Panel II – temporal R_2 concentration changes in the presence of Ade = 2.0 mM and variable concentration of ADA: (i) 0.015 U ml^{-1}, (ii) 0.025 U ml^{-1}, (iii) 0.035 U ml^{-1} (conversion of the fluorescence changes displayed in panel I by the appropriate calibration curve, Fig. S7). Panel III – catalytic rates corresponding to the production of R_2 in the presence of Ade = 2.0 mM, and variable ADA concentrations: (i) 0.015 U ml^{-1}, (ii) 0.025 U ml^{-1}, (iii) 0.035 U ml^{-1} (first order time-dependent derivatives of the curves shown in panel II). Inset: peak rates of transient formation of R_2 at different Ade concentrations. In all experiments, N_m/T_m = 0.2 μM, P_m = 0.2 μM, NTPs = 3 mM, T7 RNAP = 1.2 U μl^{-1}. Data are means ±SD, N = 3.

panel II. The temporal catalytic rates (first order derivatives) of the transcription machinery, in the presence of different Ade concentrations, are displayed in panel III. Dissipative, transient catalytic rates revealing peak rates (V_{max}) controlled by concentrations of Ade are observed (inset, panel III). Fig. 5D, panel I depicts the temporal fluorescence changes associated with R_2 transcription, in the presence of variable ADA concentrations, and a fixed concentration of Ade = 2.0 mM. As the concentration of ADA increases, the maximal fluorescence level is lower. Fig. 5D, panel II shows the temporal concentration changes of the transcribed R_2, and panel III displays the temporal catalytic rates of the transcription machinery. As the

concentration of ADA increases V_{max} lowers and the dissipative depletion of the transcription process is faster (inset, panel III). These results are consistent with the faster depletion of the allosteric Ade/aptamer subunits stabilized transcription template, as the concentration of ADA increases.

Conclusions

The study introduced allosteric ligand/aptamer complexes as functional structures orchestrating dynamic or transient catalytic DNA-based frameworks. These included the melamine (Mel)/aptamer subunits allosteric activation of the Mg^{2+}-ion-dependent DNAzyme, the allosteric inhibition of thrombin and the allosteric operation of a transcription machinery. Moreover, by coupling the allosteric ligand/aptamer complex induced stabilization of the catalytic transformation to an auxiliary enzyme depleting the ligand, the transient, dissipative, operation of catalytic transformations was demonstrated. This was exemplified by the allosteric adenosine (Ade)/aptamer complex control over fibrinogenesis or transcription machineries and the transformation of these processes into dissipative and transient pathways in the presence of adenosine deaminase (ADA). Beyond mimicking native processes by synthetic circuits, such as transcription factor guided transcription machineries, the systems might be used for amplified sensing and biomedical applications, such as dose-controlled fibrinogenesis (blood coagulation) or a biomarker-induced synthesis of RNA inhibiting aptamers. The significance of the study rests, however, on the potential generalization of the allosteric stabilization concept of DNAzyme or transcription therapeutic circuits by other ligands, and particularly designing applications of such frameworks. Besides the use of Mel or Ade as allosteric activators of DNAzymes, protein biomarkers (*e.g.*, VEGF[43]) or specific miRNAs could promote the allosteric biomarker-driven cleavage of mRNAs leading to autonomous gene therapy (for example, inducing cancer cell apoptosis by specific miRNAs).[96] Also, biomarker triggered transcription machineries could be extended to miRNA or protein-stabilized transcription templates synthesizing pre-designed aptamers with therapeutic inhibiting functions.[97] Furthermore, the transient operation of allosterically-driven DNA circuits could be extended to miRNA driven allosteric frameworks, using RNase H as the catalytic agent or by implementing other ligand/enzyme couples such as xanthine[90]/xanthine oxidase or uric acid[91]/uricase (applicable for Gout-related inflammation) or acetylcholine[92]/acetylcholinesterase (for the temporal treatment of neural diseases). Moreover, at present, all systems were operated in homogeneous solutions. Integration of the circuits within liposomes could yield functional circuit-loaded synthetic cells-protocells,[93–95] and fusion between the liposomes and native cells could provide versatile means to deliver the loads into the cells thereby signaling cell functions by artificial circuits.[50]

Author contributions

I. Willner and J. Dong designed the experiments and supervised the research. D. Froim carried out the experiments and conducted corresponding data analysis. H. Amartely contributed to the modules' characterization experiments. E. Pikarsky provided valuable insights to the topic of research. All authors reviewed and approved the final manuscript.

Conflicts of interest

The authors declare no competing financial interests.

Data availability

The data supporting this article have been included as part of the supplementary information (SI). Supplementary information: reagents, instrumentation, experimental methods, calibration curves and ITC data. See DOI: https://doi.org/10.1039/d5sc09098a.

Acknowledgements

The research was supported by the Israel Science Foundation (ISF) Precision Medicine Program, Grant No. 1696/20.

References

1 R. Nussinov, Introduction to Protein Ensembles and Allostery, *Chem. Rev.*, 2016, **116**, 6263–6266.
2 J. Liu and R. Nussinov, Allostery: An overview of its history, concepts, methods, and applications, *PLoS Comput. Biol.*, 2016, **12**, e1004966.
3 J. Monod, *Chance and Necessity: Essay on the Natural Philosophy of Modern Biology*, Vintage Books, New York, 1972.
4 S. E. Osborne and A. D. Ellington, Nucleic acid selection and the challenge of combinatorial chemistry, *Chem. Rev.*, 1997, **97**, 349–370.
5 M. Famulok and G. Mayer, Aptamer modules as sensors and detectors, *Acc. Chem. Res.*, 2011, **44**, 1349–1358.
6 J. Lee, G. Stovall and A. Ellington, Aptamer therapeutics advance, *Curr. Opin. Chem. Biol.*, 2006, **10**, 282–289.
7 F. C. Simmel, B. Yurke and H. R. Singh, Principles and applications of nucleic acid strand displacement reactions, *Chem. Rev.*, 2019, **119**, 6326–6369.
8 D. Y. Zhang and G. Seelig, Dynamic DNA nanotechnology using strand-displacement reactions, *Nat. Chem.*, 2011, **3**, 103–113.
9 D. Y. Zhang, A. J. Turberfield, B. Yurke and E. Winfree, Engineering Entropy-Driven reactions and networks catalyzed by DNA, *Science*, 2007, **318**, 1121–1125.
10 G. F. Joyce, Directed evolution of nucleic acid enzymes, *Annu. Rev. Biochem.*, 2004, **73**, 791–836.
11 R. R. Breaker and G. F. Joyce, A DNA enzyme that cleaves RNA, *Chem. Biol.*, 1994, **1**, 223–229.
12 S. K. Silverman, In vitro selection, characterization, and application of deoxyribozymes that cleave RNA, *Nucleic Acids Res.*, 2005, **33**, 6151–6163.
13 S. V. Park, J.-S. Yang, H. Jo, B. Kang, S. S. Oh and G. Y. Jung, Catalytic RNA, ribozyme, and its applications in synthetic biology, *Biotechnol. Adv.*, 2019, **37**, 107452.

14 P. Travascio, Y. Li and D. Sen, DNA-enhanced peroxidase activity of a DNA aptamer-hemin complex, *Chem. Biol.*, 1998, **5**, 505–517.
15 A. F. Fagbemi, B. Orelli and O. D. Schärer, Regulation of endonuclease activity in human nucleotide excision repair, *DNA Repair*, 2011, **10**, 722–729.
16 P. Gao, H. Yang, K. R. Rajashankar, Z. Huang and D. J. Patel, Type V CRISPR-Cas Cpf1 endonuclease employs a unique mechanism for crRNA-mediated target DNA recognition, *Cell Res.*, 2016, **26**, 901–913.
17 J. Bath, S. J. Green and A. J. Turberfield, A Free-Running DNA motor powered by a nicking enzyme, *Angew. Chem., Int. Ed.*, 2005, **44**, 4358–4361.
18 Z. Li, J. Wang and I. Willner, Autoinhibited transient, gated, and cascaded dynamic transcription of RNAs, *Sci. Adv.*, 2022, **8**, eabq5947.
19 Y. Weizmann, M. K. Beissenhirtz, Z. Cheglakov, R. Nowarski, M. Kotler and I. Willner, A virus spotlighted by an autonomous DNA machine, *Angew. Chem., Int. Ed.*, 2006, **45**, 7384–7388.
20 N. C. Seeman and H. F. Sleiman, DNA nanotechnology, *Nat. Rev. Mater.*, 2017, **3**, 17068.
21 F. Wang, X. Liu and I. Willner, DNA switches: From principles to applications, *Angew. Chem., Int. Ed.*, 2014, **54**, 1098–1129.
22 S. G. Harroun, C. Prévost-Tremblay, D. Lauzon, A. Desrosiers, X. Wang, L. Pedro and A. Vallée-Bélisle, Programmable DNA switches and their applications, *Nanoscale*, 2018, **10**, 4607–4641.
23 X. Liu, C.-H. Lu and I. Willner, Switchable reconfiguration of nucleic acid nanostructures by Stimuli-Responsive DNA machines, *Acc. Chem. Res.*, 2014, **47**, 1673–1680.
24 J. Bath and A. J. Turberfield, DNA nanomachines, *Nat. Nanotechnol.*, 2007, **2**, 275–284.
25 F. Hong, F. Zhang, Y. Liu and H. Yan, DNA Origami: scaffolds for creating higher order structures, *Chem. Rev.*, 2017, **117**, 12584–12640.
26 T. Tørring, N. V. Voigt, J. Nangreave, H. Yan and K. V. Gothelf, DNA origami: a quantum leap for self-assembly of complex structures, *Chem. Soc. Rev.*, 2011, **40**, 5636.
27 J. Li, A. A. Green, H. Yan and C. Fan, Engineering nucleic acid structures for programmable molecular circuitry and intracellular biocomputation, *Nat. Chem.*, 2017, **9**, 1056–1067.
28 G. Seelig, D. Soloveichik, D. Y. Zhang and E. Winfree, Enzyme-Free Nucleic Acid Logic Circuits, *Science*, 2006, **314**, 1585–1588.
29 L. Yue, S. Wang, Z. Zhou and I. Willner, Nucleic acid based constitutional Dynamic networks: From basic principles to applications, *J. Am. Chem. Soc.*, 2020, **142**, 21577–21594.
30 E. Del Grosso, E. Franco, L. J. Prins and F. Ricci, Dissipative DNA nanotechnology, *Nat. Chem.*, 2022, **14**, 600–613.
31 Z. Li, J. Wang and I. Willner, Transient Out-of-Equilibrium nucleic Acid-Based dissipative networks and their applications, *Adv. Funct. Mater.*, 2022, **32**, 2200799.
32 K. Jiao, B. Zhu, L. Guo, H. Zhou, F. Wang, X. Zhang, J. Shi, Q. Li, L. Wang, J. Li and C. Fan, Programming switchable transcription of topologically constrained DNA, *J. Am. Chem. Soc.*, 2020, **142**, 10739–10746.
33 P. Zhang, A. Fischer, Y. Ouyang, Y. S. Sohn, R. Nechushtai, J. Zhang, H. Tian, C. Fan and I. Willner, Topologically switchable and gated transcription machinery, *Chem. Sci.*, 2022, **13**, 10555–10565.
34 S. Xie, L. Qiu, L. Cui, H. Liu, Y. Sun, H. Liang, D. Ding, L. He, H. Liu, J. Zhang, Z. Chen, X. Zhang and W. Tan, Reversible and quantitative photoregulation of target proteins, *Chem*, 2017, **3**, 1021–1035.
35 Y. Biniuri, G.-F. Luo, M. Fadeev, V. Wulf and I. Willner, Redox-Switchable binding properties of the ATP–Aptamer, *J. Am. Chem. Soc.*, 2019, **141**, 15567–15576.
36 E. Golub, H. B. Albada, W.-C. Liao, Y. Biniuri and I. Willner, Nucleoapzymes: Hemin/G-Quadruplex DNAzyme–Aptamer Binding Site Conjugates with Superior Enzyme-like Catalytic Functions, *J. Am. Chem. Soc.*, 2015, **138**, 164–172.
37 Y. Ouyang, P. Zhang and I. Willner, Dynamic catalysis guided by nucleic acid networks and DNA nanostructures, *Bioconjugate Chem.*, 2022, **34**, 51–69.
38 Z. Huang, D. Wang, Q. Zhang, Y. Zhang, R. Peng and W. Tan, Leveraging Aptamer-Based DNA nanotechnology for bioanalysis and cancer therapeutics, *Acc. Mater. Res.*, 2024, **5**, 438–452.
39 I. Willner and M. Zayats, Electronic Aptamer-Based sensors, *Angew. Chem., Int. Ed.*, 2007, **46**, 6408–6418.
40 H.-M. Meng, H. Liu, H. Kuai, R. Peng, L. Mo and X.-B. Zhang, Aptamer-integrated DNA nanostructures for biosensing, bioimaging and cancer therapy, *Chem. Soc. Rev.*, 2016, **45**, 2583–2602.
41 C. Ji, J. Wei, L. Zhang, X. Hou, J. Tan, Q. Yuan and W. Tan, Aptamer–Protein interactions: From regulation to biomolecular detection, *Chem. Rev.*, 2023, **123**, 12471–12506.
42 W.-H. Chen, G.-F. Luo, M. Vázquez-González, R. Cazelles, Y. S. Sohn, R. Nechushtai, Y. Mandel and I. Willner, Glucose-Responsive Metal–Organic-Framework nanoparticles act as "Smart" Sense-and-Treat carriers, *ACS Nano*, 2018, **12**, 7538–7545.
43 E. W. M. Ng, D. T. Shima, P. Calias, E. T. Cunningham, D. R. Guyer and A. P. Adamis, Pegaptanib, a targeted anti-VEGF aptamer for ocular vascular disease, *Nat. Rev. Drug Discovery*, 2006, **5**, 123–132.
44 B. Deng, Y. Lin, C. Wang, F. Li, Z. Wang, H. Zhang, X.-F. Li and X. C. Le, Aptamer binding assays for proteins: The thrombin example—A review, *Anal. Chim. Acta*, 2014, **837**, 1–15.
45 J. Achenbach, W. Chiuman, R. Cruz and Y. Li, DNAZymes: From creation in vitro to application in vivo, *Curr. Pharm. Biotechnol.*, 2004, **5**, 321–336.
46 E. Golub, R. Freeman and I. Willner, A Hemin/G-Quadruplex acts as an NADH oxidase and NADH peroxidase mimicking DNAzyme, *Angew. Chem., Int. Ed.*, 2011, **50**, 11710–11714.
47 E. Golub, H. B. Albada, W.-C. Liao, Y. Biniuri and I. Willner, Nucleoapzymes: Hemin/G-Quadruplex DNAzyme–Aptamer

Binding Site Conjugates with Superior Enzyme-like Catalytic Functions, *J. Am. Chem. Soc.*, 2015, **138**, 164–172.
48 N. Lin, Y. Ouyang, Y. Qin, O. Karmi, Y. S. Sohn, S. Liu, R. Nechushtai, Y. Zhang, I. Willner and Z. Zhou, Spatially localized Entropy-Driven evolution of nucleic Acid-Based constitutional dynamic networks for intracellular imaging and spatiotemporal programmable gene therapy, *J. Am. Chem. Soc.*, 2024, **146**, 20685–20699.
49 Z. Tang, Y. Liu, M. He and W. Bu, Chemodynamic therapy: tumour Microenvironment-Mediated Fenton and Fenton-like reactions, *Angew. Chem., Int. Ed.*, 2018, **58**, 946–956.
50 Y. Ouyang, Y. S. Sohn, X. Chen, R. Nechushtai, E. Pikarsky, F. Xia, F. Huang and I. Willner, Adenosine-Triggered dynamic and transient Aptamer-Based networks integrated in liposome protocell assemblies, *J. Am. Chem. Soc.*, 2025, **147**, 19282–19295.
51 C. Gu, T. Lan, H. Shi and Y. Lu, Portable detection of melamine in milk using a personal glucose meter based on an in vitro selected Structure-Switching Aptamer, *Anal. Chem.*, 2015, **87**, 7676–7682.
52 C. Gu, Y. Xiang, H. Guo and H. Shi, Label-free fluorescence detection of melamine with a truncated aptamer, *Analyst*, 2016, **141**, 4511–4517.
53 Q. Li, P. Song and J. Wen, Melamine and food safety: a 10-year review, *Curr. Opin. Food Sci.*, 2019, **30**, 79–84.
54 E. D. C. Domingo, A. A. Tireli, C. A. Nunes, A. V. Batista, M. C. Guerreiro and S. M. Pinto, Rapid extraction of melamine in powdered milk for direct electrospray ionization tandem mass spectrometry analysis, *Talanta*, 2014, **132**, 535–540.
55 A. M. R. Mondal, A. Desmarchelier, E. Konings, R. Acheson-Shalom and T. Delatour, Liquid Chromatography−Tandem Mass Spectrometry (LC−MS/MS) method extension to quantify simultaneously melamine and cyanuric acid in egg powder and soy protein in addition to milk products, *J. Agric. Food Chem.*, 2010, **58**, 11574–11579.
56 P. Ma, H. Guo, Y. Zhang and Z. Wang, A novel CRISPR/Cas14a1-Exo III aptasensor for melamine detection coupled with systematically studied binding mechanism of truncated aptamer, *Sens. Actuators, B*, 2022, **374**, 132847.
57 U.S. Food and Drug Administration, Chemical Contaminants, Archived from the original on January 11, 2017, https://wayback.archive-it.org/7993/20170111174251/http://www.fda.gov/Food/FoodborneIllnessContaminants/ChemicalContaminants/ucm164520.htm, accessed October 2025.
58 J. C. Chapin and K. A. Hajjar, Fibrinolysis and the control of blood coagulation, *Blood Rev.*, 2014, **29**, 17–24.
59 R. I. Litvinov and J. W. Weisel, Blood clot contraction: Mechanisms, pathophysiology, and disease, *Res. Pract. Thromb. Haemostasis*, 2023, **7**, 100023.
60 A. S. Wolberg, Fibrinogen and fibrin: synthesis, structure, and function in health and disease, *J. Thromb. Haemostasis*, 2023, **21**, 3005–3015.
61 M. Di Nisio, S. Middeldorp and H. R. Büller, Direct thrombin inhibitors, *N. Engl. J. Med.*, 2005, **353**, 1028–1040.
62 S. Zhao, R. Tian, J. Wu, S. Liu, Y. Wang, M. Wen, Y. Shang, Q. Liu, Y. Li, Y. Guo, Z. Wang, T. Wang, Y. Zhao, H. Zhao, H. Cao, Y. Su, J. Sun, Q. Jiang and B. Ding, A DNA origami-based aptamer nanoarray for potent and reversible anticoagulation in hemodialysis, *Nat. Commun.*, 2021, **12**, 358.
63 C. Riccardi, E. Napolitano, C. Platella, D. Musumeci and D. Montesarchio, G-quadruplex-based aptamers targeting human thrombin: Discovery, chemical modifications and antithrombotic effects, *Pharmacol. Ther.*, 2020, **217**, 107649.
64 J. Dong and I. Willner, Transient transcription machineries modulate dynamic functions of G-Quadruplexes: temporal regulation of biocatalytic circuits, gene replication and transcription, *Angew. Chem., Int. Ed.*, 2023, **62**, e202307898.
65 Y. Ouyang, J. Dong and I. Willner, Dynamic DNA Networks-Guided directional and orthogonal transient biocatalytic cascades, *J. Am. Chem. Soc.*, 2023, **145**, 22135–22149.
66 I. Simon, J. Barnett, N. Hannett, C. T. Harbison, N. J. Rinaldi, T. L. Volkert, J. J. Wyrick, J. Zeitlinger, D. K. Gifford, T. S. Jaakkola and R. A. Young, Serial regulation of transcriptional regulators in the yeast cell cycle, *Cell*, 2001, **106**, 697–708.
67 D. Accili and K. C. Arden, FOXOS at the crossroads of cellular metabolism, differentiation, and transformation, *Cell*, 2004, **117**, 421–426.
68 G. L. Hager, J. G. McNally and T. Misteli, Transcription dynamics, *Mol. Cell*, 2009, **35**, 741–753.
69 T. E. Sztal and D. Y. R. Stainier, Transcriptional adaptation: a mechanism underlying genetic robustness, *Development*, 2020, **147**, dev186452.
70 J. M. Vaquerizas, S. K. Kummerfeld, S. A. Teichmann and N. M. Luscombe, A census of human transcription factors: function, expression and evolution, *Nat. Rev. Genet.*, 2009, **10**, 252–263.
71 T. L. Lenstra, J. Rodriguez, H. Chen and D. R. Larson, Transcription dynamics in living cells, *Annu. Rev. Biophys.*, 2016, **45**, 25–47.
72 T. I. Lee and R. A. Young, Transcriptional regulation and its misregulation in disease, *Cell*, 2013, **152**, 1237–1251.
73 S. A. Ament, J. R. Pearl, J. P. Cantle, R. M. Bragg, P. J. Skene, S. R. Coffey, D. E. Bergey, V. C. Wheeler, M. E. MacDonald, N. S. Baliga, J. Rosinski, L. E. Hood, J. B. Carroll and N. D. Price, Transcriptional regulatory networks underlying gene expression changes in Huntington's disease, *Mol. Syst. Biol.*, 2018, **14**, e7435.
74 G. Ragazzon and L. J. Prins, Energy consumption in chemical fuel-driven self-assembly, *Nat. Nanotechnol.*, 2018, **13**, 882–889.
75 R. P. Goodman, M. Heilemann, S. Doose, C. M. Erben, A. N. Kapanidis and A. J. Turberfield, Reconfigurable, braced, three-dimensional DNA nanostructures, *Nat. Nanotechnol.*, 2008, **3**, 93–96.
76 J. Wang, Z. Li and I. Willner, Dynamic reconfigurable DNA nanostructures, networks and materials, *Angew. Chem., Int. Ed.*, 2023, **62**, e202215332.
77 Z. Zhou, Y. Ouyang, J. Wang and I. Willner, Dissipative gated and cascaded DNA networks, *J. Am. Chem. Soc.*, 2021, **143**, 5071–5079.

78 J. Wang, Z. Li, Z. Zhou, Y. Ouyang, J. Zhang, X. Ma, H. Tian and I. Willner, DNAzyme- and light-induced dissipative and gated DNA networks, *Chem. Sci.*, 2021, **12**, 11204–11212.
79 C. Wang, L. Yue and I. Willner, Controlling biocatalytic cascades with enzyme–DNA dynamic networks, *Nat. Catal.*, 2020, **3**, 941–950.
80 E. Del Grosso, G. Ragazzon, L. J. Prins and F. Ricci, Fuel-Responsive allosteric DNA-Based aptamers for the transient release of ATP and cocaine, *Angew. Chem., Int. Ed.*, 2019, **58**, 5582–5586.
81 Y. Ouyang, P. Zhang, H. Manis-Levy, Y. Paltiel and I. Willner, Transient dissipative optical properties of aggregated AU nanoparticles, CDSE/ZNS quantum dots, and supramolecular nucleic Acid-Stabilized AG nanoclusters, *J. Am. Chem. Soc.*, 2021, **143**, 17622–17632.
82 F. Spitz and E. E. M. Furlong, Transcription factors: from enhancer binding to developmental control, *Nat. Rev. Genet.*, 2012, **13**, 613–626.
83 H. M. Petrykowska, C. M. Vockley and L. Elnitski, Detection and characterization of silencers and enhancer-blockers in the greater CFTR locus, *Genome Res.*, 2008, **18**, 1238–1246.
84 A. Travers, Transcriptional switches: the role of mass action, *Phys. Life Rev.*, 2004, **1**, 57–69.
85 M. Weitz, J. Kim, K. Kapsner, E. Winfree, E. Franco and F. C. Simmel, Diversity in the dynamical behaviour of a compartmentalized programmable biochemical oscillator, *Nat. Chem.*, 2014, **6**, 295–302.
86 S. W. Schaffter and R. Schulman, Building in vitro transcriptional regulatory networks by successively integrating multiple functional circuit modules, *Nat. Chem.*, 2019, **11**, 829–838.
87 M. Sun, J. Deng and A. Walther, Communication and Cross-Regulation between Chemically Fueled Sender and Receiver Reaction Networks, *Angew. Chem., Int. Ed.*, 2022, **62**, e202214499.
88 Z. Li, J. Wang and I. Willner, Alternate strategies to induce dynamically modulated transient transcription machineries, *ACS Nano*, 2023, **17**, 18266–18279.
89 D. E. Huizenga and J. W. Szostak, A DNA aptamer that binds adenosine and ATP, *Biochemistry*, 1995, **34**, 656–665.
90 Y. Ding, L. Gu, X. Wang, Z. Zhang, H. Zhang and J. Liu, Affinity-Guided coevolution of aptamers for guanine, xanthine, hypoxanthine, and adenine, *ACS Chem. Biol.*, 2024, **19**, 208–216.
91 Y. Liu and J. Liu, Selection of DNA aptamers for sensing uric acid in simulated tears, *Anal. Sens.*, 2022, **2**, e202200010.
92 J. G. Bruno, M. P. Carrillo, T. Phillips and B. King, Development of DNA aptamers for cytochemical detection of acetylcholine, *In Vitro Cell. Dev. Biol. Anim.*, 2008, **44**, 63–72.
93 B. C. Buddingh and J. C. M. Van Hest, Artificial Cells: Synthetic Compartments with Life-like Functionality and Adaptivity, *Acc. Chem. Res.*, 2017, **50**, 769–777.
94 W. Jiang, Z. Wu, Z. Gao, M. Wan, M. Zhou, C. Mao and J. Shen, Artificial cells: past, present and future, *ACS Nano*, 2022, **16**, 15705–15733.
95 T. Trantidou, M. Friddin, Y. Elani, N. J. Brooks, R. V. Law, J. M. Seddon and O. Ces, Engineering compartmentalized biomimetic micro- and nanocontainers, *ACS Nano*, 2017, **11**, 6549–6565.
96 P. Zhang, L. Yue, M. Vázquez-González, Z. Zhou, W.-H. Chen, Y. S. Sohn, R. Nechushtai and I. Willner, MicroRNA-Guided Selective Release of Loads from Micro-/Nanocarriers Using Auxiliary Constitutional Dynamic Networks, *ACS Nano*, 2020, **14**, 1482–1491.
97 N. Que-Gewirth and B. Sullenger, Gene therapy progress and prospects: RNA aptamers, *Gene Ther.*, 2007, **14**, 283–291.